JACS
JOURNAL OF THE AMERICAN CHEMICAL SOCIETY

Communication

pubs.acs.org/JACS

Evidence for Helical Structure in a Tetramer of α2-8 Sialic Acid: Unveiling a Structural Antigen

Marcos D. Battistel,[†] Michael Shangold,[†] Loc Trinh,[‡] Joseph Shiloach,[‡] and Darón I. Freedberg*[,†,‡]

[†]Laboratory of Bacterial Polysaccharides, Center for Biologics Evaluation and Research, Food and Drug Administration, 1401 Rockville Pike, Rockville, Maryland 20852-1448, United States

[‡]Biotechnology Unit, MSC 5522, National Institute of Diabetes and Digestive and Kidney Diseases, National Institutes of Health, Bethesda, Maryland 20892, United States

Supporting Information

ABSTRACT: Characteristic H-bonding patterns define secondary structure in proteins and nucleic acids. We show that similar patterns apply for α2-8 sialic acid (SiA) in H_2O and that H-bonds define its structure. A $^{15}N,^{13}C$ α2-8 SiA tetramer, $(SiA)_4$, was used as a model system for the polymer. At 263 K, we detected intra-residue through-H-bond *J* couplings between ^{15}N and C8 for residues R-I–R-III of the tetramer, indicating H-bonds between the ^{15}N's and the O8's of these residues. Additional *J* couplings between the ^{15}N's and C2's of the adjacent residues confirm the putative H-bonds. NH groups showing this long-range correlation also experience slower $^{1}H/^{2}H$ exchange. Additionally, detection of couplings between H7 and C2 for R-II and R-III implies that the conformations of the linkers between these residues are different than in the monomers. These structural elements are consistent with two left-handed helical models: 2 residues/turn (2_4 helix) and 4 residues/turn (1_4 helix). To discriminate between models, we resorted to $^{1}H,^{1}H$ NOEs. The 2_4 helical model is in better agreement with the experimental data. We provide direct evidence of H-bonding for $(SiA)_4$ and show how H-bonds can be a determining factor for shaping its 3D structure.

The capsular polysaccharides (PSs) of *Neisseria meningitidis* and *Escherichia coli* K1 are crucial virulence factors that enable the organisms to survive in human serum[1a] and to colonize the meninges,[1b,c] resulting in the development of meningococcal disease. Among *N. meningitidis* serogroups (A, B, C, W-135, X, and Y), the capsular PS of serogroup B, composed of α2-8 sialic acid (SiA), shows unique immunogenic properties and elicits a weak immune response compared to the A, C, W-135, and Y PSs.[2a−c] Binding to its cognate antibody requires 10 or more SiA residues,[2c] not the usual 6−7;[2d] thus, α2-8 polysialic acid (PSA) is thought to adopt a helical conformation in solution, yielding a structural epitope.[2d] There is widespread agreement that α2-8 PSA forms a helix in solution, but there is no consensus on the type of helix.[3] Proposed helical models are based on complementarity of the PS with its cognate antibody,[3d] sparse NMR data,[3a,b] and/or simulations,[3e] but to date there is no *direct* evidence for a helical structure. Here we report direct observation of H-bonds, which alone supports a helix in a tetramer of α2-8 sialic acid, $(SiA)_4$, at 263 K. Experimental heteronuclear *J* couplings and inter-residue NOEs reinforce this structure.

Chart 1. Chemical Structure of α2-8 $(SiA)_4$, with W-Coupling, Where Detected, Highlighted in Red

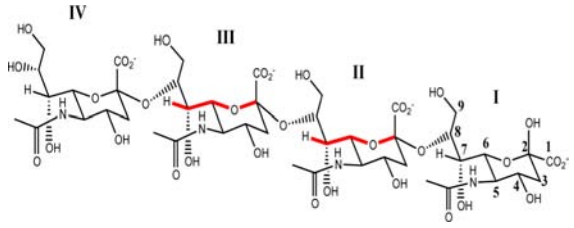

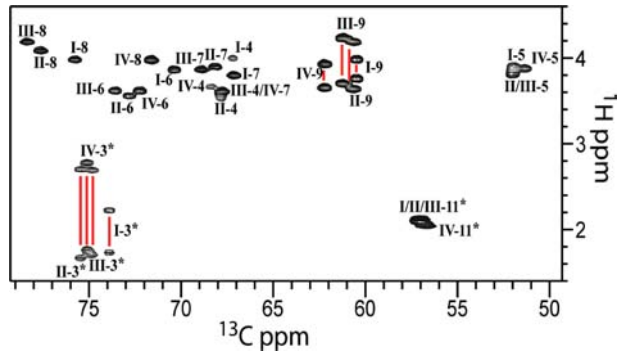

Figure 1. $^{1}H,^{13}C$-HSQC spectrum of $(SiA)_4$, collected at 263 K and pH 6.5 (20 mM Na_2HPO_4). Roman numerals indicate residue position, and Arabic numerals indicate atom position.

Solution NMR structure determination of α2-8 PSA is hampered by signal degeneracy[4] and the lack of suitable tools for carbohydrate structural characterization. To overcome these difficulties and increase the number of NMR experiments that can be used in structure determination, we enriched the sample in ^{15}N and ^{13}C. We studied $^{15}N,^{13}C$-labeled $(SiA)_4$ (Chart 1) because nearly all its signals are well resolved, enabling unambiguous resonance assignment. The $^{1}H,^{13}C$ HSQC spectrum of $(SiA)_4$ (Fig. 1) provides a set of well-resolved cross-peaks, especially those corresponding to atoms at positions 3, 6, 8, and 9. Thus, NMR experiments on $(SiA)_4$ enable the detection and unambiguous assignment of through-

Received: January 19, 2012
Published: June 15, 2012

dx.doi.org/10.1021/ja300624j | J. Am. Chem. Soc. 2012, 134, 10717−10720

bond and through-space correlations. We further increased the number of NMR experiments available to us by collecting NMR data of $(SiA)_4$ in ^1H_2O (as opposed to ^2H_2O) to utilize the amide HN in SiA as a probe for structural information.

Secondary structure in proteins and nucleic acids is stabilized via characteristic H-bond patterns. It is plausible that H-bonding shapes carbohydrate structures as well. We hypothesized that, by searching for H-bonds, we would identify important structural elements for carbohydrate structure determination. Secondary structure can be inferred from NMR on the basis of *direct* evidence, via the detection of a long-range scalar coupling between the H-bonded nuclei,[5] or *indirect* evidence, such as NOEs[6a] and slow $^1H/^2H$ exchange rates.[6b] Direct detection of H-bonds was reported for proteins and nucleic acids.[5,7] Indirect evidence for H-bonding in carbohydrates has been presented,[8] but to our knowledge no through-H-bond correlation was directly detected by NMR for carbohydrates in H_2O.

SiA residues have several functional groups for H-bonding: one N-acetyl group, in which the HN group can be a donor, and two carbonyl groups that can be acceptors, one at C1 and the other at C10. Internal SiA residues in $(SiA)_4$ have five O atoms that can participate in H-bonds: three in hydroxyl groups at C4, C7, and C9, one forming the glycosidic linkage at C8, and one part of the pyranose ring at C6. All these carbons also bear H atoms (Chart 1). We thus used a CBCANH experiment,[9] modified to detect small J couplings, to probe the tetramer for long-range $^{13}C-^{15}N$ J couplings (Fig. 2A).

The ^{15}N's of residues R-I–R-III show an unexpected intra-residue correlation to C8. A similar long-range correlation is absent for residue R-IV (Fig. 2A) and for the monomer (Fig. S1), suggesting that the proposed H-bond is a structural feature intrinsic to the tetramer. Thus, we hypothesized that the ^{15}N-to-C8 coupling implies the presence of a H-bond. If such an intra-residue H-bond is present, there should also exist an inter-residue correlation between the HN and the C2 of a contiguous

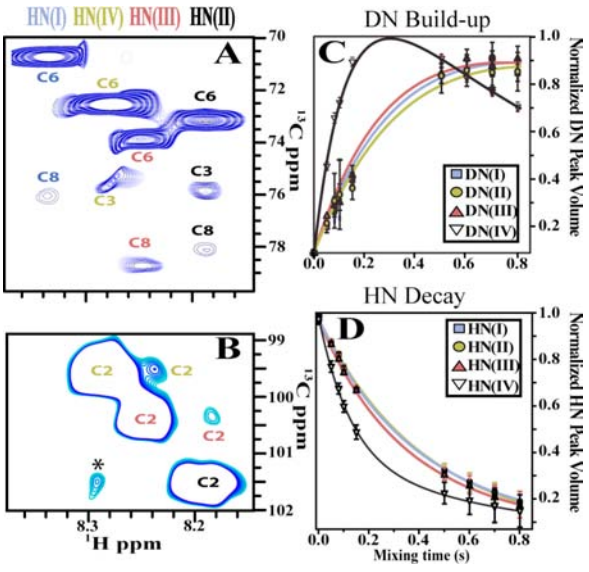

Figure 2. NMR experiments for H-bond detection (263 K, pH* 6.5). (A) Long-range CBCANH; correlations to different $(SiA)_4$ residues are color coded based on residue position. (B) Long-range HNC2 on $(SiA)_4$; * denotes an impurity. SOLEXSY DN buildup (C) and HN decay (D) traces obtained for each $(SiA)_4$ residue. The data were fitted to extract exchange rate constants presented in Table 1.

Table 1. Exchange Rates, Protection Factors, and W-Coupling Constants Measured at 263 K

residue	k_{HD} (Hz)	β PF[a]	α PF[b]	$^4J_{H7\text{-}C2}$ (Hz)
R-I	0.90 ± 0.12	3.33	3.79	n.c.[c]
R-II	1.28 ± 0.33	2.34	2.66	0.8 ± 0.5
R-III	0.77 ± 0.28	3.90	4.43	1.5 ± 0.5
R-IV	3.41 ± 0.06	0.88	1.00	n.c.[c]

[a]PF relative to SiA. [b]PF relative to R-IV. [c]No correlation.

residue. We detected such correlations for R-II and R-III (Fig. 2B) via a long-range HNC2 experiment adapted from an HNCO experiment by exciting C2 resonances rather than CO.[5a] Thus, the existence of a H-bond between the HN and O8 is reinforced.

H-bonds in the HN groups of R-I–R-III should reduce the $^1H/^2H$ exchange rates for these HN's. Indeed, we observe decreased $^1H/^2H$ exchange rates in $(SiA)_4$, via SOLEXSY experiments,[10a,b] ideal for $(SiA)_4$ because it targets $^1H/^2H$ exchange rates of 0.5–20 s^{-1}. The measurement of $^1H/^2H$ exchange rates helps identify nascent helices in disordered proteins,[10b] where secondary structure elements are transient. It should also help in carbohydrates, which are thought to have partly disordered structures. Residues involved in secondary structure typically yield HN protection factors (PFs)[10c] between 2 and 5.[10b] We monitored peak intensities as a function of mixing time and fitted them to obtain exchange rate constants[10a] (Figs. 2C,D and S1, and Table 1). HN's of R-I–R-III exchange ~3-fold slower than R-IV, as expected for H-bonded HN's. We used SiA monomer (β configuration) $^1H/^2H$ exchange rate as an external control to obtain a PF for each SiA residue (Table 1). R-IV in the tetramer displays a PF close to unity, and thus behaves as a free SiA monomer whose HN is less protected from exchange. Conversely, HN's for internal residues in $(SiA)_4$ are more protected from exchange. Thus, we use R-IV's HN as an internal reference for the PFs in the remaining HN's in different sections of the $(SiA)_4$ chain, as it is in the α configuration and thus more representative of similar residues in the oligomer. Together, the results from CBCANH and SOLEXSY experiments indicate that the structure of $(SiA)_4$ stems from an intra-residue H-bonding pattern that repeats for each of the first three residues of the molecule (Fig. S1).

An H-bond between a HN and O8 implies that conformations favoring the proximity between the lone pair of electrons of O8 and HN are preferred. Fulfillment of this requirement should translate into a restricted flexibility of the glycerol chain. Rigidification of the chain is further supported by heteronuclear coupling constants between the ^1H at position 7 and the ^{13}C at position 2 ($^4J_{H7\text{-}C2}$, Table 1), analogous to $^1H-^1H$ W-coupling.[11a] W-couplings are present in rigid systems, where the arrangement of the bonds separating the pair of coupled nuclei is coplanar and resembles a W (Chart 1). W-couplings are common in pyranose rings, where the chair conformation enables the W arrangement to be adopted.[11b] However, conformations that break this coplanar arrangement can decrease or obliterate this long-range coupling.[11b]

Such $^4J_{H7\text{-}C2}$ couplings have been proposed from DFT calculations[12a] but not measured experimentally in αSiA. In contrast, we observed W-couplings only for R-II and R-III via HSQMBC[12b] in unlabeled $(SiA)_4$. This suggests that the monomer's glycerol chain (atoms 7–9) adopts a different conformation than R-I in $(SiA)_4$ and may be modulated by anomeric configuration. This coupling indicates that the H7-

dx.doi.org/10.1021/ja300624j | J. Am. Chem. Soc. 2012, 134, 10717–10720

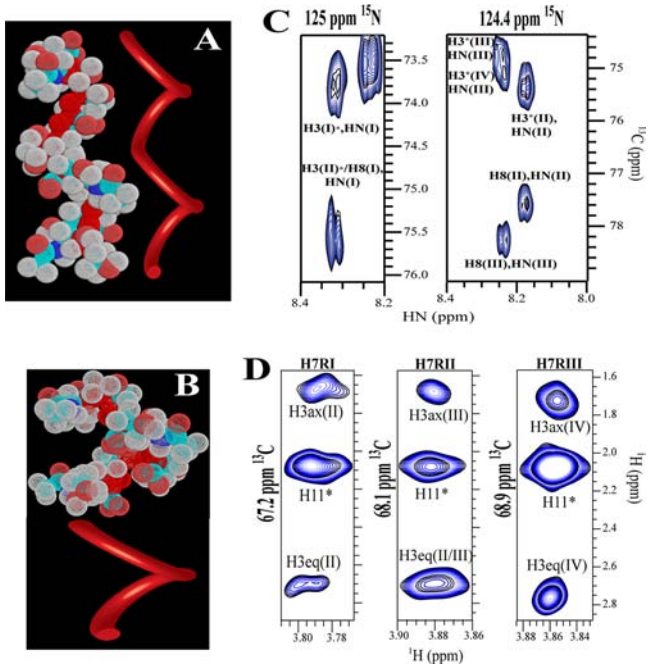

Figure 3. (A,B) Static side-view models for $(SiA)_4$ consistent with the data: helical models with (A) 2 and (B) 4 residues/turn. Ribbons depict the trace followed by the oligosaccharide backbone. (C) CNH-NOESY: intra- and inter-residue NOEs between amide H and ring H atoms. (D) ^{1}H,^{13}C-HSQC-NOESY: NOEs between the H7's of each of the first three residues and H3's of a contiguous residue.

C7-C6-H6 torsion is ~90°, as H7 must adopt a coplanar or quasi-coplanar W conformation with C2 to be measurable.[12a] Based on the above results, we generated non-energy-minimized, *static* models for $(SiA)_4$ (Fig. 3), in which O8 of R-I−R-III is H-bonded intra-residually to the HN, and H7's are W-coupled to their own C2 in a quasi-coplanar arrangement. Interestingly, forcing the linker between residues, C6(i)-C7(i)-C8(i)-O8(i)-C2(i+1), into a conformation required to form both a W arrangement between H7−C2 and a H-bond (O8−HN <3 Å apart) rendered two of the three torsional angles of the linker chain fixed. Rotations about the C2(i+1)−O8(i) bond led to conformations that resulted in atom clashes. These restraints also imply two possible structural models for $(SiA)_4$ with no clashes: left-handed helix 2_4, with 2, or helix 1_4, with 4 residues/turn (Fig. 3A,B). It is also noteworthy that glycosidic torsions in the 1_4 model are consistent with the *exo* anomeric effect, while those in the 2_4 helix are not. Nonetheless, this finding indicates that the tetramer forms a helix.

We used NOEs to probe for helical structure and distinguish between the two helical models. The CNH-NOE[13] and ^{1}H,^{13}C HSQC-NOESY experiments (Fig. 3) yielded intra- and inter-residue correlations. The results of these experiments agree with $(SiA)_4$ adopting a helical conformation and support the 2_4 more strongly than the 1_4 helix. We observed NOEs only for R-I−R-III between H7, H8, and H9 and both H3's of the following residue. We also observed cross-peaks between HN and the intra-residue H8 and the inter-residue H3's (Table S1). These NOEs indicate that the oligomer is not in a fully extended conformation, but in a more compact one, where two contiguous residues twist, bringing H3 and H7, and H8 and H9, less than 5 Å apart. Moreover, the H7's of R-I−R-III show a strong intra-residue correlation to the H11's, consistent with a conformation required to observe a W-coupling between H7 and C2, and the H3 to H8 inter-residue NOEs are consistent with H-bonding between O8 and the HN. The fact that 29 inter-residue NOEs (~7 for each residue) were observed is very unusual for carbohydrates and provides strong evidence for structure. Additionally, these sequential NOEs recur in R-I−R-III, reinforcing the notion of a restricted glycosidic linkage of a defined and periodic structure. Comparison of experimental and predicted NOEs yields the following: For the 2_4 helix, 71% of the predicted inter-residues NOEs were observed experimentally, but all of the experimental NOEs agree with the model. For the 1_4 helix, only 53% of the predicted intra-residue NOEs were observed, and as many as 4 of the 29 NOEs disagree with this model (Tables S1 and S2). The agreement between the NOE data and the 2_4 helix is striking. Equally striking is the small number of experimental constraints necessary to generate this helical model: merely three H-bonds and two W-couplings. These atomic constraints induce a left-handed helix in solution. This conclusion is supported by previously unreported ^{1}H,^{1}H NOEs and a slower ^{1}H/^{2}H exchange rate for the three first residues in the tetramer.

Our results for $(SiA)_4$ at 263 K have several important implications: First, even short oligomers like the one used in these experiments can adopt a helical structure in solution. Second, H-bonding in α2-8 PSA may be of great importance in defining the overall PS structure by stabilizing the glycosidic conformation and consequently defining the observed helix. By limiting the degrees of freedom of the glycosidic linkage, H-bonding appears to be a determining factor for shaping the α2-8 $(SiA)_4$ molecular topology. Third, the 2_4 left-handed helix contains 2 residues/turn. While the left-handedness of this helix is consistent with predictions, the pitch is not.[3b−e] Only one study identifies a 2.2 residue/turn helix as a subpopulation of other conformations in α2-8 $(SiA)_3$ (trimer). Woods et al.[3e] predicted a model using NOEs and J coupling data collected from a trimer and selected a cluster of conformations from MD simulations that agreed with their measurements. A helix was obtained when propagating the trimer structure, in good agreement with the 2_4 $(SiA)_4$ model, highlighting the potential for NMR-MD symbiosis for structure determination in carbohydrates. However, as previously observed, 10 residues are required to span the antibody combining site, which would require longer stretches of oligomers to adopt a conformation similar to that of the polymer.[4] Thus, the helix observed in the tetramer may differ from that of larger oligomers. Nonetheless, we propagated both helices to a decamer and docked them with mAb735[3d] (Fig. S2). Preliminary data suggest that the 2_4 model fits better in the binding site because it establishes more contacts than the 1_4 model. Affinity of IgM^{NOV7} for poly(A) and PSA is not explained with the 2_4 helix proposed herein because it disagrees with the poly(A) model. This may be due to structural reorganization on binding, as suggested by experiments that show a higher entropy cost for mAb735 binding to longer oligomers. Thus, models derived in the absence of mAb735 may differ from those of the free form. More research will verify if the $(SiA)_4$ conformation resembles that of the decamer.

The original work on α2-8 SiA's[3b,d] set the stage for the present structural characterization, but the results presented here disagree with the previously proposed models that were based on sparse NMR data. One model was built from torsional angles extracted from NMR ($^{3}J_{HH}$ couplings) and using the mAb735 binding site as a target, where the helical model contained 6 residues/turn.[3d] Another helical model,[3b] based

dx.doi.org/10.1021/ja300624j | J. Am. Chem. Soc. 2012, 134, 10717−10720

mainly on coupling constants and NOE data from the polymer, suggested 3−4 residues/turn. These types of studies are complicated because no restraints can be extracted for individual residues as a result of spectral overlap. NOEs can result from intra-residue correlations, from a residue that is contiguous, or from a sequentially remote residue, but it is difficult to distinguish intra- from inter-residue NOEs due to signal degeneracy. Moreover, angles extracted from coupling constants are not only a result of conformational averaging of a single residue but may result from conformational averages of different residues. One major difference between the present and previous studies is the availability of fully ^{15}N,^{13}C-enriched SiA oligomers that enabled us to utilize and optimize protein-type NMR methods in determining carbohydrate structure. These methods could not have been used in previous studies since many were not developed at the time. In addition, isotopic labeling increased the sensitivity and resolution of the present NMR experiments and is currently catalyzing the development of carbohydrate-tailored NMR experiments.[14]

In summary, we present *direct* evidence of H-bonding, via through-H-bond $^{3}J_{NC}$ correlations, in an oligosaccharide chain in solution. These results agree with $(SiA)_4$ adopting a left-handed helix in solution. H-bonding and W-coupling data are consistent with two left-handed helical models obtained by varying the O6(i)−C8(i−1) angle: 2_4, with 2 residues/turn, and 1_4, with 4 residues/turn. NOEs obtained from ^{1}H,^{13}C HSQC-NOESY yield distances in agreement with a 2_4 helix and rule out the 1_4 helix under the current experimental conditions. This conclusion is supported by previously unreported ^{1}H,^{1}H NOEs and a slower $^{1}H/^{2}H$ exchange rate for the three first residues in the tetramer. We hope that this discovery will facilitate the determination of carbohydrate structures in solution via the detection of H-bonding. Our results could also provide information that was previously unavailable, aid in the refinement of carbohydrate force fields, and give clues regarding secondary structure in carbohydrates.

Secondary structure in carbohydrates may facilitate protein recognition by optimizing carbohydrate/protein contacts and may favor binding by preorganizing the bound conformation. If the H-bond pattern presented in this report can be extrapolated to larger oligomers, H-bonds can have a cooperative effect in stabilizing the structure. The evidence presented for $(SiA)_4$ and preliminary temperature-dependent studies (unpublished) suggest that the H-bonds reported herein are transient and may induce dynamic formation of helices. This behavior, on one hand, will ensure a structural epitope formed along the chain at a given time and, on the other hand, may increase the avidity of the ligand by having multiple propagating helical stretches. The data presented herein demonstrate that helical $(SiA)_4$ is a low-energy conformation at 263 K; at higher temperatures, this helix is likely in equilibrium with other conformations and will be present in solution even if not directly observed. If it resembles the structural epitope, the antibody will selectively bind the helix. H-bond detection is of extreme importance in a structural world that appears to be dominated by averages. It may lead to unveiling structural patterns in glycans, to discovering secondary structure, and to structure/function studies that could catalyze the deciphering of the "sugar code".

■ ASSOCIATED CONTENT

Supporting Information

Experimental details and characterization data. This material is available free of charge via the Internet at http://pubs.acs.org.

■ AUTHOR INFORMATION

Corresponding Author

daron_freedberg@nih.gov

Notes

The authors declare no competing financial interest.

■ ACKNOWLEDGMENTS

We thank Dr. D. A. Torchia and Dr. W. F. Vann for helpful discussions and V. Chevelkov help with SOLEXSY.

■ REFERENCES

(1) (a) Hill, D. J.; Griffiths, N. J.; Borodina, E.; Virji, M. *Clin. Sci.* **2010**, *118*, 547. (b) Echenique-Rivera, H.; Muzzi, A.; Tordello, E. D.; Seib, K. L.; Francois, P.; Rappuoli, R.; Pizza, M.; Serruto, D. *PLOS Pathogens* **2011**, *7*, e10020271. (c) Kim, K. J.; Elliott, S. J.; Cello, F. D.; Stins, M. F.; Kim, K. S. *Cell Microbiol.* **2003**, *5*, 245.

(2) (a) Wyle, F. A.; Tramont, E. C.; Lowentha, J.; Berman, S. L.; Brandt, B. L.; Altieri, P. L.; Artenste, M.; Kasper, D. L. *J. Infect. Dis.* **1972**, *126*, 514. (b) Finne, J.; Leinonen, M.; Makela, P. H. *Lancet* **1983**, *2*, 355. (c) Jennings, H. J.; Roy, R.; Michon, F. *J. Immunol.* **1985**, *134*, 2651. (d) Kabat, E. A.; Liao, J.; Osserman, E. F.; Gamian, A.; Michon, F.; Jennings, H. J. *J. Exp. Med.* **1988**, *168*, 699.

(3) (a) Henderson, T. J.; Venable, R. M.; Egan, W. *J. Am. Chem. Soc.* **2003**, *125*, 2930. (b) Yamasaki, R.; Bacon, B. *Biochemistry* **1991**, *30*, 851. (c) Brisson, J. R.; Baumann, H.; Imberty, A.; Perez, S.; Jennings, H. J. *Biochemistry* **1992**, *31*, 4996. (d) Evans, S. V.; et al. *Biochemistry* **1995**, *34*, 6737. (e) Yongye, A. B.; Gonzalez-Outeirino, J.; Glushka, J.; Schultheis, V.; Woods, R. J. *Biochemistry* **2008**, *47*, 12493.

(4) Michon, F.; Katzenellenbogen, E.; Kasper, D. L.; Jennings, H. J. *Biochemistry* **1987**, *26*, 476.

(5) (a) Cordier, F.; Grzesiek, S. *J. Am. Chem. Soc.* **1999**, *121*, 1601. (b) Dingley, A. J.; Grzesiek, S. *J. Am. Chem. Soc.* **1998**, *120*, 8293.

(6) (a) Wagner, G.; Kumar, A.; Wuthrich, K. *Eur. J. Biochem.* **1981**, *114*, 375. (b) Wagner, G.; Wuthrich, K. *J. Mol. Biol.* **1979**, *134*, 75.

(7) (a) Dingley, A. J.; Masse, J. E.; Peterson, R. D.; Barfield, M.; Feigon, J.; Grzesiek, S. *J. Am. Chem. Soc.* **1999**, *121*, 6019. (b) Wang, Y. X.; Jacob, J.; Cordier, F.; Wingfield, P.; Stahl, S. J.; Lee-Huang, S.; Torchia, D.; Grzesiek, S.; Bax, A. *J. Biomol. NMR* **1999**, *14*, 181.

(8) (a) Sheng, S. Q.; Vanhalbeek, H. *Biochem. Biophys. Res. Commun.* **1995**, *215*, 504. (b) Norris, S. E.; Landström, J.; Bull, A. W. T. E.; Widmalm, G.; Freedberg, D. I. *Biopolymers* **2011**, *97*, 145. (c) Sandström, C.; Baumann, H.; Kenne, L. *J. Chem. Soc., Perkins Trans. 2* **1998**, 2385. (d) Langeslay, D. J.; Young, R. P.; Beni, S.; Beecher, C. N.; Mueller, L. J.; Larive, C. K. *Glycobiology* **2012**, in press.

(9) Grzesiek, S.; Bax, A. *J. Magn. Reson.* **1992**, *91*, 201.

(10) (a) Chevelkov, V.; Xue, Y.; Rao, D. K.; Forman-Kay, J. D.; Skrynnikov, N. R. *J. Biomol. NMR* **2010**, *46*, 227. (b) Yao, J.; Chung, J.; Eliezer, D.; Wright, P. E.; Dyson, H. J. *Biochemistry* **2001**, *40*, 3561. (c) Molday, R. S.; Englander, S. W.; Kallen, R. G. *Biochemistry* **1972**, *11*, 150.

(11) (a) Sternhell, S. *Rev. Pure Appl. Chem.* **1964**, *14*, 15. (b) Pan, Q. F.; Klepach, T.; Carmichael, I.; Reed, M.; Serianni, A. S. *J. Org. Chem.* **2005**, *70*, 7542.

(12) (a) Klepach, T.; Zhang, W. H.; Carmichael, I.; Serianni, A. S. *J. Org. Chem.* **2008**, *73*, 4376. (b) Williamson, R. T.; Marquez, B. L.; Gerwick, W. H.; Kover, K. E. *Magn. Reson. Chem.* **2000**, *38*, 265.

(13) Diercks, T.; Coles, M.; Kessler, H. *J. Biomol. NMR* **1999**, *15*, 177.

(14) Barb, A.; Freedberg, D.; Battistel, M.; Prestegard, J. *J. Biomol. NMR* **2011**, *51*, 163.